4-29-2008

Magnetic properties of one-dimensional Ni/Cu and Ni/Al multilayered nanowires: Role of nonmagnetic spacers

Partha Pratim Pal
Michigan Technological University

Ranjit Pati
Michigan Technological University

Magnetic properties of one-dimensional Ni/Cu and Ni/Al multilayered nanowires: Role of nonmagnetic spacers

Partha Pratim Pal and Ranjit Pati*
Department of Physics, Michigan Technological University, Houghton, Michigan 49931, USA
(Received 19 December 2007; revised manuscript received 1 April 2008; published 29 April 2008)

We have used density functional theory within spin-polarized local density approximation to investigate the equilibrium structure, electronic, and magnetic properties of one-dimensional Ni/Cu and Ni/Al multilayered nanowires. In particular, we look into the subtle changes in the magnetic properties of the nanowires with the change in the width of the nonmagnetic spacer. Our calculations yield the magnitude of cohesive energy in both the systems to decrease with the increase in the concentration of the nonmagnetic spacer, suggesting that Ni rich nanowires are more stable. Analysis of the magnetic moment per Ni atom (μ_{av}) in the Ni/Cu hybrid multilayered nanowire suggests that there is a steady decrease in μ_{av} with the increase in the number of Cu layers. In contrast, in Ni/Al multilayered nanowire, there is a nonmonotonic decrease in μ_{av} with the increase in Al layers. The observed difference in magnetic property between Ni/Cu and Ni/Al multilayered nanowires is attributed to the dissimilar interfacial bonding in the two cases. In the case of Ni/Al nanowire, the nonmonotonic variation in μ_{av} is due to the strong directional nature of the Ni *d* and Al *p* hybridization, which favors Ni to have higher coordination number. Higher coordination for Ni leads to smaller μ_{av} in the Ni/Al multilayered nanowire. However, the hybridization between Ni *d* and Cu *s* states is predominantly responsible for the smaller μ_{av} in the Ni/Cu nanowire. Furthermore, we found that in Ni/Al multilayered nanowire with two Al spacer layer, the antiferromagnetic configuration is favored over ferromagnetic configuration. In Ni/Cu multilayered nanowire, ferromagnetic configuration is favored over antiferromagnetic configuration for the same spacer length.

DOI: 10.1103/PhysRevB.77.144430 PACS number(s): 75.70.Cn, 71.15.Mb, 73.22.−f, 73.20.−r

I. INTRODUCTION

Since the past two decades, the magnetic and electronic properties of multilayered heterostructures with alternating magnetic and nonmagnetic layers have been the focus of intense research for their multifunctional applications ranging from magnetic sensors to memory alloys. The origin of this research goes back to as early as 1985 when Grünberg and co-workers[1,2] discovered the role of nonmagnetic spacer in tuning the interlayer exchange coupling (IEC) between two neighboring magnetic layers. Subsequently, giant magnetoresistance (GMR) was simultaneously discovered by Baibich *et al.*[3] and Binasch *et al.*,[4] followed by the detection of oscillations in IEC with varying width of the nonmagnetic spacer.[5] These seminal works[1–5] form the basis of present day's computer hard disks and other magnetic storage devices.[6] In the past few years, the demand for smaller, lighter, and ultrahigh density memory devices has prompted researchers to look for novel low-dimensional materials.[7–9] In this regard, one-dimensional (1D) multilayered magnetic nanowire has shown considerable promise.

Various groups have been successful in developing techniques for controlled growth of these multilayered nanowires. For example, Blondel *et al.*[7] observed 14% GMR in Co/Cu/Co multilayered nanowire. By using nanopore template, Chien *et al.*[10] reported the fabrication of Ni nanowires with diameters in the range of 5 nm–10 μm. Stress induced martensitic phase transformation in Ni/Al hybrid nanowire has also been reported.[11] It has been found that Ni/Al nanowire has the potential to outperform bulk Ni/Al as a shape memory alloy.[11] Fabrications of Co/Cu multilayered nanowire with ~350 repetitions of Co/Cu sequences have also been reported.[12] Using altogether a different approach based on lithography, Urazhdin *et al.*[13] reported the fabrication of $Ni_{84}Fe_{16}/Cu(Pt)/Ni_{84}Fe_{14}$ multilayered nanopillars and demonstrated the current driven switching in the nanopillars. Single crystalline Ni/Cu nanowire has also been fabricated[14] by electrodepositing them into anodic alumina membranes. Very recently, by using programmable template-assisted deposition technique, Choi *et al.*[15] mass fabricated Co/Pt multisegment nanowire with well-defined magnetic and nonmagnetic layer widths—renewing strong interest in multilayered nanostructures. Despite these experimental progresses in fabrication[7–9,12–15] and characterization of multilayered magnetic nanowire, only limited attention has been given to understanding the most crucial atomic scale structural heterogeneity of the magnetic multilayered nanowires and its role in modulating the magnetic properties of the nanowire. However, it should be noted that bulk multilayered system has been extensively studied by Bruno,[16] Stoeffler and Gautier,[17] van Schilfgaarde and Herman,[18] and Lang *et al.*[19]

In the present paper, we have concentrated on 1D Ni/Cu and Ni/Al multilayered nanowires in the strong confinement regime and have used first-principles approach to look into the subtle changes in the magnetic and electronic properties of the wire with the change in the width of the nonmagnetic spacer. In particular, we address how the atomic level structural heterogeneity at the interface affects their magnetic property. We have performed periodic density functional calculation within the local spin density approximation (LSDA)[20] to probe the compositional dependent magnetic and electronic properties of the nanowires. The Vienna *ab initio* simulation code (VASP)[21] that uses plane wave basis function and ultrasoft pseudopotential to describe the

valence-core interaction is utilized for our calculation. The calculated cohesive energies per atom (E_c) in both the nanowires are found to increase with the increase in the concentration of the nonmagnetic spacer, suggesting that Ni rich nanowires are more stable. Analysis of the magnetic moment per Ni atom (μ_{av}) in the Ni/Cu hybrid multilayered nanowire suggests that there is a steady decrease in μ_{av} with the increase in the number of Cu layers. In contrast, in the Ni/Al multilayered nanowire, there is a nonmonotonic decrease in μ_{av} with the increase in Al layers. For certain concentration of Al, particularly for three and six layers in the nine layer unit cell, a sudden drop in μ_{av} is found. The observed difference in magnetic property between Ni/Cu and Ni/Al multilayered nanowires is ascribed to the dissimilar interfacial bonding in the two cases. In case of Ni/Al nanowire, the nonmonotonic variation in μ_{av} is due to the strong directional nature of the Ni *d* and Al *p* hybridization, which favors Ni to have higher coordination number. The higher the Ni coordination number in the Ni/Al multilayered nanowire, the smaller the μ_{av}. However, in the Ni/Cu nanowire, the hybridization between Ni *d* and Cu *s* states is predominantly responsible for the smaller μ_{av}. Furthermore, we found that in Ni/Al multilayered nanowire with two Al spacer layer, the antiferromagnetic configuration is favored over ferromagnetic configuration. In Ni/Cu multilayered nanowire, ferromagnetic configuration is favored over antiferromagnetic configuration for the same spacer length.

The rest of the paper is organized as follows. A brief computational procedure is described in Sec. II with results and discussions in Sec. III. In Sec. IV, we have summarized our results with a brief conclusion.

II. COMPUTATIONAL PROCEDURE

Since no prior information is available on the atomic level structural details of the multilayered nanowires under consideration, we recourse to bulk geometry as guiding structures to construct the Ni/Cu and Ni/Al nanowires. First, we construct the pristine Ni nanowire along the closely packed (111) direction of the fcc lattice of Ni. Then, we have selected nine layers having 39 atoms (733733733) with *ABCABCABC* packing from the *ABCABCABC*$\cdots$ series and have placed them in a tetragonal unit cell with a lattice parameter of 18.18 Å along the wire axis to construct the supercell for the nanowire. The other two sides of the tetragonal unit cell are taken to be 15 Å long to guarantee negligible interaction between nanowire and its image along the *x* and *y* directions. The hybrid Ni/Cu and Ni/Al multilayered nanowires are then created by layer wise substitution of Ni with Cu and Al, respectively, starting from the last layer of the unit cell. The reason for considering Cu and Al as nonmagnetic spacers is to avoid significant lattice mismatch at the interface as both of them have same fcc bulk structure as that of Ni. Furthermore, Ni/Cu nanowires have been shown to preserve fcc phase[14] of the Ni-Cu bulk alloy. Although Ni-Al bulk alloy has been reported to prefer *B*2 phase (CsCl type)[22–26] over the $L1_0$ phase, to the best of our knowledge, no structural information has been reported in Ni/Al nanowire. Geng *et al.*[27] performed spin-polarized generalized gradient approximation (GGA) corrected density functional calculations on bulk Ni-Al alloy with varying composition and reported that the alloy has a lower cohesive energy in its *B*2 phase as compared to the $L1_0$ phase with a 50% concentration of both Ni and Al. Since the one-dimensional structures in the strong confinement regime considered here are expected to be less sensitive to the choice of *k* points used to sample the Brillouin zone and considering the computational limitation involving higher *k* point mesh, we have used $1\times1\times1$ *k*-point mesh within the Monkhorst–Pack (MP) scheme for the determination of equilibrium nanowire structures. The structures are considered optimized when the force on individual atom is less or equal to 0.01 eV/Å. The convergence criterion for energy during the self-consistent calculation is taken to be 10^{-6} eV. To determine the electronic and magnetic properties of the nanowires, we use a finer, $1\times1\times1$ *k*-point mesh within the MP scheme to sample the Brillouin zone. We have also tested the convergence of the electronic structure property in a representative nanowire ($Ni_{10}Cu_{29}$) by increasing the $1\times1\times11$ *k*-point mesh to $1\times1\times15$ *k*-point mesh in MP scheme and found almost no change in the energy band structure. The LSDA approach is utilized for our calculation. Although spin-polarized GGA is expected to be more accurate than LSDA, we found the GGA approach to overestimate the magnetic moment. For example, in the case of GGA, the well-known fcc Fe is found to be ferromagnetic at 0 K, which is in disagreement with the experimental result. However, LSDA approach is found to give the correct magnetic state. Spin precession and spin-orbit interaction effects are not taken into account in our calculation. We have used Wigner Seitz radii of 2.43, 2.48, and 2.65 a.u. for Ni, Cu, and Al, respectively, to determine the local magnetic moments on individual atoms. The cutoff for the plane wave is taken to be 237.6 eV and is kept fixed during calculations of all the multilayered nanowires.

III. RESULTS AND DISCUSSIONS

A. Equilibrium nanowire structures and stability

The optimized pristine and multilayered structures are presented in Fig. 1. No significant structural differences are noted between the pristine Ni and Cu nanowires. This can be understood from the fact that the difference in bulk lattice constants of Ni (3.52 Å) (Ref. 28) and Cu (3.61 Å) (Ref. 28) is small. Both wires after structural optimization more or less preserve their fcc (111) directional lattice symmetry, with a small but noticeable structural relaxation in the *A* layer only due to confinement effect, which lead to both contraction and expansion in Ni-Ni and Cu-Cu bond lengths compared to their interatomic distances of 2.49 and 2.56 Å, respectively, in the bulk phase. For the Ni/Cu multilayered nanowire, as expected, no significant structural difference from their pristine counterpart is found. However, in the case of pristine Al nanowire, the loss of fcc translational symmetry is clearly evident from the strong contraction and expansion tendency of the interatomic distances in the wire. We find that the interatomic distances in the Al nanowire varies from 2.49 to 3.01 Å. Interatomic distance in bulk fcc Al is

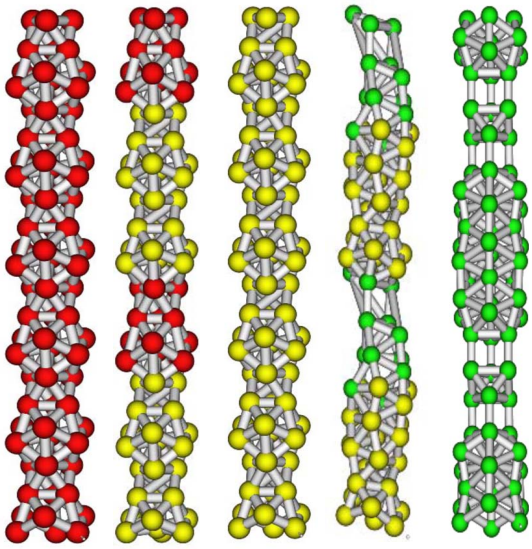

(a) (b) (c) (d) (e)

FIG. 1. (Color online) Optimized (a) Cu_{39}, (b) $Ni_{26}Cu_{13}$, (c) Ni_{39}, (d) $Ni_{26}Al_{13}$, and (e) Al_{39} nanowire structures. Two unit cells are shown. Notation: red (dark gray), Cu; yellow (light gray), Ni; and dark green (dark gray), Al.

2.86 Å.[28] More intriguing effects are found in Ni/Al multilayered nanowires. For example, in the three [Fig. 1(d)] layers of Al in the Ni-Al nanowire, the apparent loss of fcc translational symmetry along the (111) direction with clustering tendency at the Ni-Al interface is clearly evident. This effect results to the expansion of Al-Al distance. For the two Al layer in the wire, the Al-Al distance varies from 2.86 to 3.20 Å. In the case of three Al layer, the Al-Al distance varies from 2.58 to 3.16 Å. For $N_{Al}=4-8$, the Al-Al distance varies from 2.64–3.01, 2.63–3.09, 2.55–2.95, 2.64–3.15, and 2.53–2.99 Å, respectively. The major structural relaxation in the Ni/Al nanowire could be understood from the nature of hybridization between Ni d and Al p states. To facilitate the strong hybridization between Ni d and Al p states and to prohibit formation of short Al-Al bonds, which are energetically more expensive,[26] Ni/Al multilayered nanowire structures undergo major structural relaxation at the interface leading to loss of fcc translational symmetry. Earlier findings also suggest that bulk Ni/Al multilayered system prefers $B2$ structure (similar to CsCl) (Refs. 22–26) over the $L1_0$ phase.[29] The former one allows Ni atom to be surrounded by more Al atoms to maximize Ni-Al interaction by facilitating Ni d and Al p hybridization.

To deduce the stability of the multilayered nanowire, we calculated the cohesive energy per atom, $E_c=(E_{NW}-\Sigma_j E_j)/N$, where E_{NW} is the energy of the nanowire, N is the total number of atoms, and E_j is the energy of the individual atom. From the calculated cohesive energy, summarized in Fig. 2, we found that the stability of both nanowires increases with increasing concentration of Ni layers. By comparing the bulk cohesive energies of Ni, Al, and Cu, we found that the Ni has the lowest cohesive energy (−4.435 eV).[28] Thus, the increase in Ni concentration leads to a much stable nanowire structure. Furthermore, it has been shown before that the bulk Ni/Al multilayered structure is less stable than the bulk Ni fcc structure.[27]

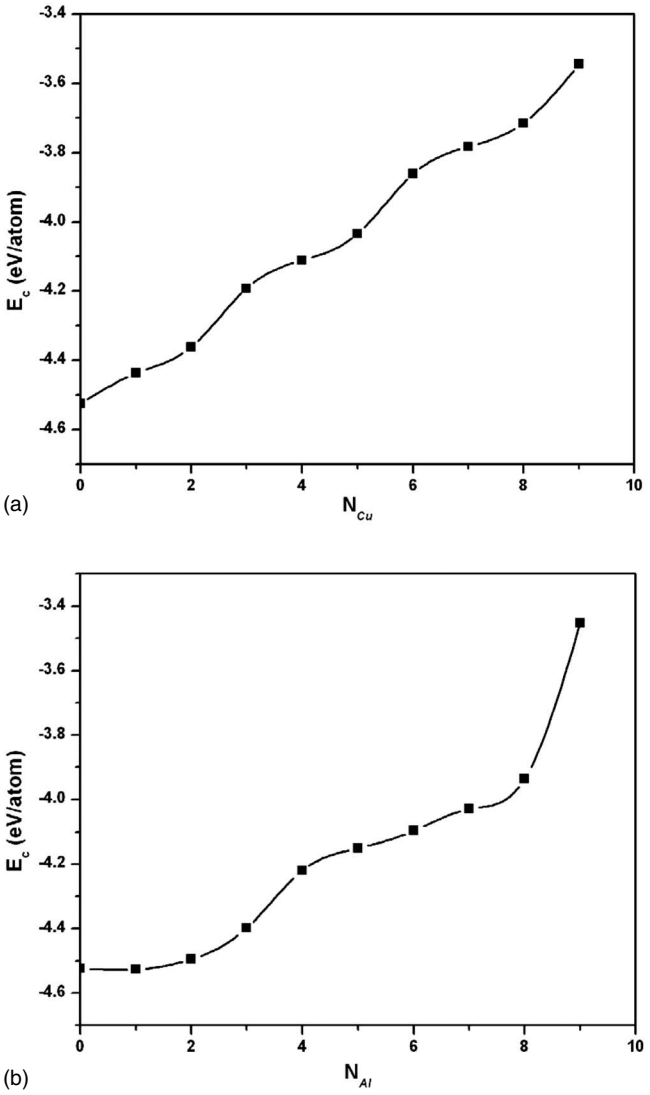

FIG. 2. Calculated cohesive energy E_c as a function of (a) number of Cu layers (N_{Cu}) in Ni/Cu multilayered nanowire and (b) number of Al layers (N_{Al}) in Ni/Al multilayered nanowire.

B. Magnetic properties of the nanowire

The average local magnetic moment (μ_{av}) per Ni atom in the multilayered nanowire is calculated as

$$\mu_{av}=\frac{\sum \mu_{Ni}}{N}, \tag{1}$$

where N is the total number of Ni atoms in the multilayered nanowire and μ_{Ni} is the magnetic moment of the Ni atom. The calculated μ_{av} as a function of nonmagnetic spacer thickness are summarized in Fig. 3. One can notice from Fig. 3 that μ_{av} in the pristine Ni nanowire is $0.59\mu_B$, reasonably in agreement with the reported values of $0.66\mu_B$ obtained in the case of Ni (111) surface. The latter result is obtained by

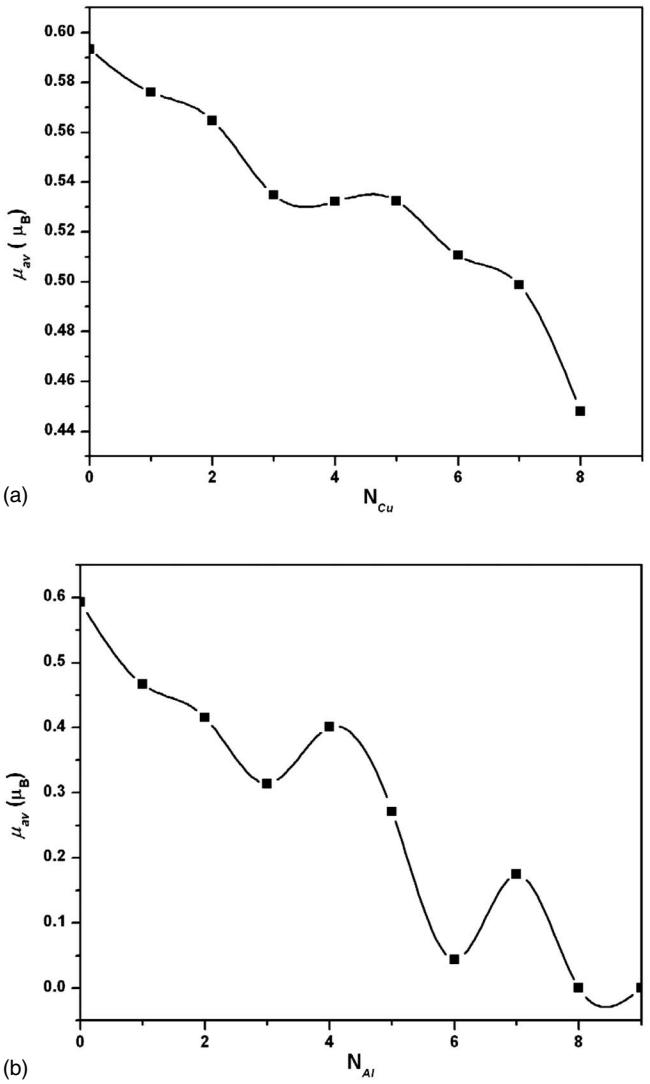

FIG. 3. Calculated magnetic moment per Ni atom (μ_{av}) as a function of (a) number of Cu layers (N_{Cu}) in Ni/Cu nanowire and (b) number of Al layers (N_{Al}) in Ni/Al nanowire.

using full potential linearized augmented plane wave method.[30] The smaller calculated magnetic moment in pristine 1D Ni nanowire compared to 2D Ni (111) surface[30] could be understood from the fact that the local density functional approach, which does not include dynamical correlation effect, underestimates the magnitude of the magnetic moment. From Fig. 3(a), a steady decrease in μ_{av} in Ni-Cu multilayered nanowire with increase in the Cu layer thickness is noted. For example, μ_{av} is found to be $0.56\mu_B$ in $Ni_{33}Cu_6$ nanowire, $0.53\mu_B$ in $Ni_{23}Cu_{16}$ nanowire, and $0.45\mu_B$ for Ni_7Cu_{32} nanowire. In contrast, a nonmonotonic variation in μ_{av} is noted in Ni/Al multilayered nanowire [Fig. 3(b)]. This contrasting magnetic behavior between Ni/Cu and Ni/Al multilayer nanowires can be understood from their atomic level structural details. In the case of Ni/Cu multilayered nanowire, we found a monotonic decrease in Ni-Ni bond length with the increase in Cu layer thickness. In the Ni/Al nanowire, the nonmonotonic variation in the magnetic moment can be ascribed to the strong directional nature of the Ni *d* and Al *p* hybridization, which favors Ni to be surrounded by more Al atoms. This, in turn, leads to the change in the interfacial arrangement of Ni and Al atoms. The layer with seven Al atoms at the Ni-Al interface provides higher coordination for Ni than the interfacial layer with three Al atoms. The seven Al atoms at the interface allow the Ni atoms to be surrounded by more Al atoms to facilitate stronger Ni *d* and Al *p* hybridization. The stronger the hybridization and the higher the Ni coordination is, the lower the magnetic moment is. Earlier electronic structure calculation in Ni cluster also revealed the sensitiveness of the magnetic moment to Ni coordination.[31] It was reported that the decreasing coordination of Ni would lead to the increase in its magnetic moment.[31] Thus, one can conclude that the quenching of magnetic moment associated with the Ni atoms in Ni/Al multilayered nanowire is directly proportional to the number of Al atoms at the Ni-Al interface. When a layer with three Ni atoms is followed by a layer with seven Al atoms, we see a considerable decrease in the magnetic moment [Fig. 3(b)]. This happens when the Ni atoms in the *A* layer of the *ABCABCABC* unit cell are replaced by Al atoms. In the Ni/Cu nanowire, primarily Cu *s* state hybridizes with Ni *d* state resulting to a decrease in the number of unoccupied Ni $d\downarrow$ states. This, in fact, explains the reduction in μ_{av} in Ni-Cu nanowire. To gain further insights into the decrease in μ_{av} in Ni-Cu nanowire, we analyzed the local magnetic moment of the Ni as well as Cu at the Ni/Cu interface and found that the Cu atom is not magnetically polarized. Similar effect was also noted for interfacial Al atom in the Ni/Al nanowire. This suggests that there is no spin-polarized electron transfer at the interface as reported in Fe-Pt hybrid nanowire.[32] The cause of the modification of the magnetic moment is ascribed to the nature of the interfacial bonding. The interfacial bonding determines the structural rearrangement of the Ni as well as the coordination of Ni in the Ni/Cu and Ni/Al nanowire and thus the magnetic moment. It should be noted that a similar calculation on Fe/Pt multilayered nanowire,[32] where Pt is strongly spin polarized at the interface, yielded opposite trend in μ_{av}, i.e., increasing trend in magnetic moment with the increase in Pt spacer thickness.

We have also used the *ABCABC* configuration along the (111) direction of the bulk fcc structure in the supercell to investigate the role of nonmagnetic spacer on the interlayer exchange coupling (*J*) in the nanowire. In the *ABCABC* unit cell, *BC* layers are the nonmagnetic spacer layers and layer *A* is the magnetic layer. The value of *J* is obtained ($=E_F - E_{AF}$) from the calculated total energy in the ferromagnetic (E_F) and antiferromagnetic configurations (E_{AF}). In the antiferromagnetic configuration, the spin on the one side of the nonmagnetic spacer is aligned in the opposite direction to that on the other side. The spin flip induced structural relaxation is explicitly taken into account during the calculation of total energy in ferromagnetic and antiferromagnetic configurations. For the two Cu layer as spacer in the Ni/Cu multilayered nanowire, we found that the ferromagnetic configuration is more stable (by 5 meV) than the corresponding antiferromagnetic configuration. In Ni/Al multilayered nanowire with two layer spacer, the antiferromagnetic configuration is found to be more stable (3.7 meV) than the corresponding ferromagnetic configuration. The stability of the antiferromagnetic configuration in Ni/Al multilayered nano-

wire suggests that the superexchange means is the dominant mechanism in the Ni/Al nanowire. The strong superexchange interaction in the Ni/Al nanowire arises from the directional character of the bonding between the Al p and Ni d states, which are similar to the bonding in MnO.[33] In contrast, a direct exchange mechanism plays a vital role in stabilizing the ferromagnetic phase in Ni/Cu multilayered nanowire. In Ni/Cu, the predominant Ni d and Cu s hybridization favors ferromagnetism. It has been previously reported that Ni/Cu bulk alloy with 46%–50% Ni concentration exhibits weak ferromagnetism at low temperatures.[34] It should also be noted that the similar order in the value of the interlayer exchange coupling has been reported[16] in bulk multilayered system. Our calculation thus clearly illustrates that the nature of nonmagnetic spacer plays an important role in modulating the interlayer exchange coupling.

C. Band structure

The spin-polarized band structure analysis of the pristine Ni nanowire (Fig. 4) shows a dominance of d character in the spin-down [Fig. 4(b)] valence bands keeping in line with the band structure of bulk Ni.[35,36] The spin-up valence bands of the same wire turn out to be a mix of s, p, and d bands [Fig. 4(a)]. As Cu starts to take over from Ni in terms of composition of the nanowire, we clearly see hybridization of Cu s, p bands with the Ni $d\downarrow$ bands around the Fermi energy (Fig. 5) as seen in a representative nanowire with seven layers of Cu [Fig. 5(b)]. The spin-up bands around the Fermi energy are mainly Cu s, p,d bands with little contribution from the Ni d bands [Fig. 5(a)]. The reduction in μ_{av} with the increase in the number of Cu layers thus can be attributed to the gradual occupation of the Ni $d\downarrow$ bands as a result of its participation in the hybridization with the Cu s, p bands. This fact will again be reinforced when we analyze the Ni d density of states of Ni/Cu nanowires with variable ratios of Ni and Cu concentration. The Ni/Al hybrid multilayered nanowire shows a strong Ni d and Al p hybridization. Previous studies have also reported directional character of Al p and Ni d bonding in Ni/Al bulk alloy.[26] The spin-up valence and conduction bands [Fig. 6(a)] are mainly mix of s, p, and d bands. The strong Ni $d\downarrow$ band and Al p hybridization can also be clearly noticed in Fig. 6(b). This hybridization leads to the partial filling of the Ni $d\downarrow$ and Ni $d\uparrow$ bands resulting to the quenching of magnetic moment (μ_{av}). A more vivid picture of Ni band filling can be obtained from the analysis of the partial density of states.

D. Partial density of states

To get a better insight into the reason behind the decrease in μ_{av} with the increase in the number of nonmagnetic spacer layers, we analyzed the partial density of states (PDOS) of each element in the nanowire. Pristine Ni nanowire shows dominance of unoccupied $d\downarrow$ states [Fig. 7(a)], near the Fermi energy which leads to the finite μ_{av}. Substitution of Ni atoms with Cu atom layer wise in the nanowire induces hybridization of the Cu s, p bands with the Ni $d\downarrow$ bands resulting to a decrease in the number of unoccupied Ni $d\downarrow$ states. This is clearly evident from the Ni d-PDOS in the representative $Ni_{10}Cu_{29}$ nanowire [Fig. 7(b)]. The increase in Cu concentration in the Ni/Cu nanowire leads to the filling of the Ni $d\downarrow$ states monotonically resulting in a steady decrease in μ_{av}. Similarly, in the Ni/Al nanowire, the increase in Al concentration leads to the partial filling of Ni $d\downarrow$ and Ni $d\uparrow$ states [Fig. 7(c)], leading to the decrease in μ_{av}. The stronger quenching of μ_{av} for certain layer composition is due to the strong directional Ni d and Al p hybridization, which favors higher coordination for Ni to maximize Ni-Al interaction.

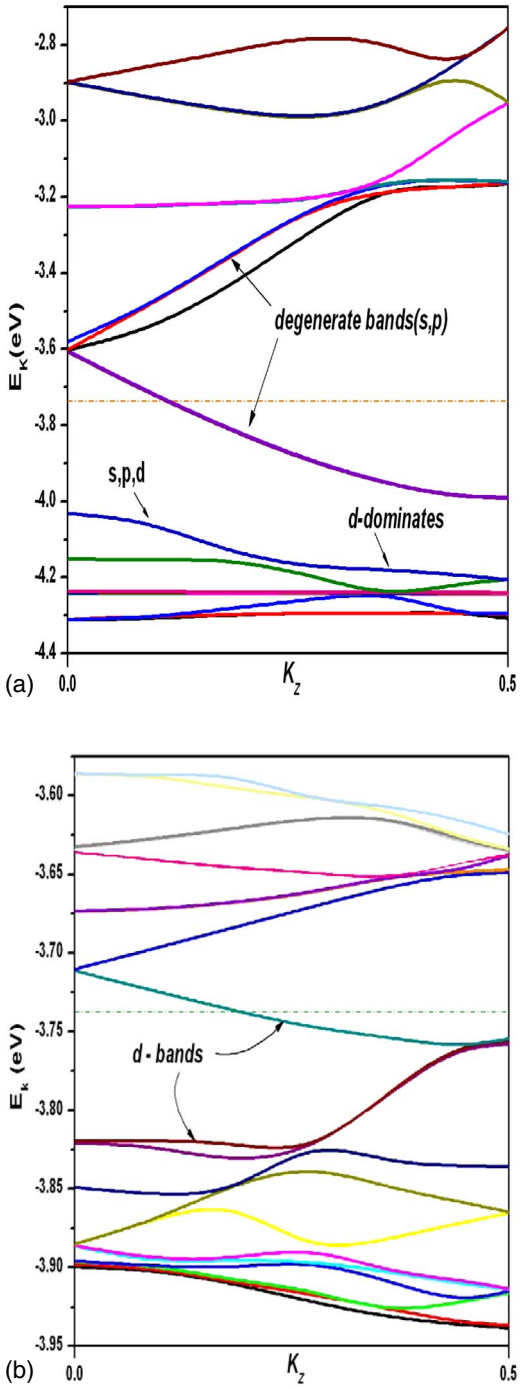

FIG. 4. (Color online) Spin-polarized band structures of pristine Ni nanowire: (a) spin up and (b) spin down. Dotted lines represent the Fermi energy.

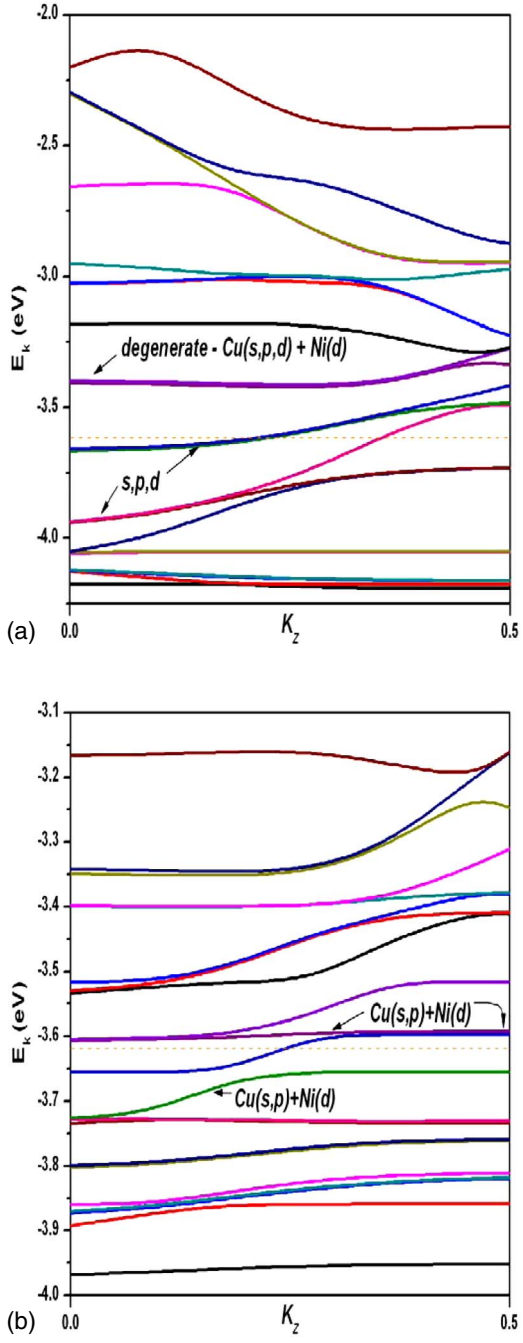

FIG. 5. (Color online) Spin-polarized band structures of $Ni_{10}Cu_{29}$ nanowire: (a) spin up and (b) spin down. Dotted lines represent the Fermi energy.

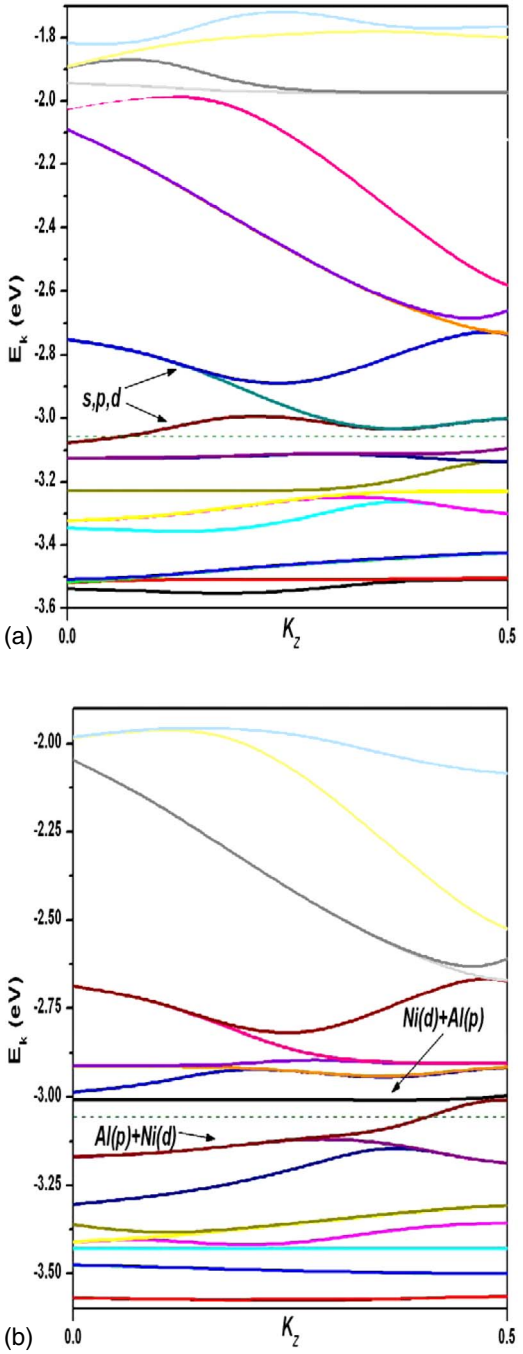

FIG. 6. (Color online) Spin-polarized band structure of $Ni_{10}Al_{29}$ nanowire: (a) spin up and (b) spin down. Dotted lines represent the Fermi energy.

Similar Ni d and B p hybridization favoring higher coordination has been reported in Ni rich Ni-B cluster.[37] It is also clearly evident from Figs. 7(b) and 7(c) that the asymmetry between spin-up and spin-down partial d-band densities of states is stronger in Ni/Cu nanowire as compared to that in Ni/Al nanowire. This explains the smaller μ_{av} in $Ni_{10}Al_{29}$ nanowire as compared to that in $Ni_{10}Cu_{29}$ nanowire.

IV. CONCLUSIONS

In summary, we have used first-principles density functional approach within LSDA to predict equilibrium structures, stability, electronic, and magnetic properties of the 1D Ni/Cu and Ni/Al multilayered nanowires. We found the Ni rich nanowires to be more stable. In Ni/Cu nanowire, a steady decrease in μ_{av} is found with the increase in Cu spacer layers. In contrast, a nonmonotonic decrease in μ_{av} with the increase in Al spacer layers is obtained in Ni/Al nanowire. The difference in magnetic property between Ni/Cu and Ni/Al nanowire is attributed to their dissimilar interfacial bonding. In Ni/Al, the directional Ni d and Al p hybridization favors Ni to have higher coordination number leading to a smaller μ_{av}. In Ni/Cu, the hybridization is be-

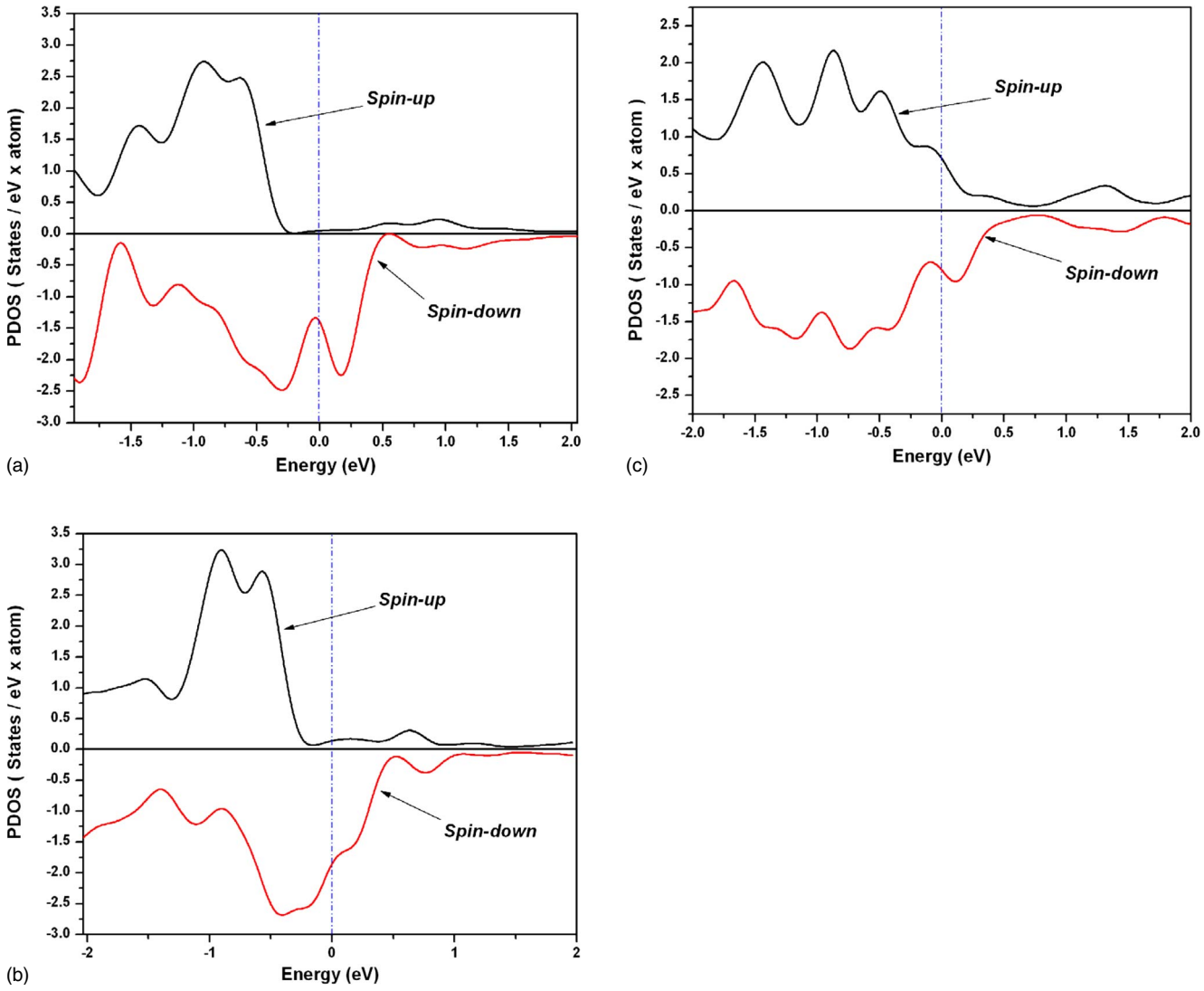

FIG. 7. (Color online) Projected spin-polarized d-band density of states (PDOS) of Ni in (a) pristine Ni nanowire, (b) $Ni_{10}Cu_{29}$ nanowire, and (c) $Ni_{10}Al_{29}$ nanowire. Spin-up PDOS is plotted on the positive axis; spin-down PDOS is plotted on the negative axis for visualization purposes. The Fermi energy lies at $E=0$.

tween Ni d and Cu s states. This hybridization leads to the reduction in the number of unoccupied Ni $d\downarrow$ states and hence results to a smaller μ_{av}. We have also found for *ABCABC* unit cell with *BC* as spacer layers that the antiferromagnetic configuration is favored over ferromagnetic configuration in Ni/Al nanowire. In the Ni/Cu nanowire, for the similar spacer configuration, the ferromagnetic configuration is favored over antiferromagnetic configuration. This study thus not only reveals the atomic level structural heterogeneity of the multilayered nanowire structures but also demonstrates the role of the nonmagnetic spacer in modulating the magnetic properties.

*patir@mtu.edu

[1] P. Grünberg, J. Appl. Phys. **57**, 3673 (1985).
[2] P. Grünberg, R. Schreiber, Y. Pang, M. B. Brodsky, and H. Sowers, Phys. Rev. Lett. **57**, 2442 (1986).
[3] M. N. Baibich, J. M. Broto, A. Fert, F. Nguyen Van Dau, F. Petroff, P. Eitenne, G. Creuzet, A. Friederich, and J. Chazelas, Phys. Rev. Lett. **61**, 2472 (1988).
[4] G. Binasch, P. Grünberg, F. Saurenbach, and W. Zinn, Phys. Rev. B **39**, 4828 (1989).
[5] S. S. P. Parkin, N. More, and K. P. Roche, Phys. Rev. Lett. **64**, 2304 (1990).
[6] G. A. Prinz, Science **282**, 1660 (1998).
[7] A. Blondel, J. P. Meier, B. Doudin, and J.-Ph. Ansermet, Appl. Phys. Lett. **65**, 3019 (1994).
[8] L. Piraux, J. M. George, J. F. Despres, C. Leroy, E. Ferain, R. Legras, K. Ounadjela, and A. Fert, Appl. Phys. Lett. **65**, 2484 (1994).
[9] M. Tanase, D. M. Silevitch, A. Hultgren, L. A. Bauer, P. C.

Searson, G. J. Meyer, and D. H. Reich, J. Appl. Phys. **91**, 8549 (2002).
[10] C. L. Chien, L. Sun, M. Tanase, L. A. Bauer, A. Hultgren, D. M. Silevitch, G. J. Meyer, P. C. Searson, and D. H. Reich, J. Magn. Magn. Mater. **249**, 146 (2002).
[11] H. S. Park, Nano Lett. **6**, 958 (2006).
[12] F. Elhoussine, L. Vila, L. Piraux, and G. Faini, J. Magn. Magn. Mater. **290-291**, 116 (2005).
[13] S. Urazhdin, W. P. Pratt, and J. Bass, J. Magn. Magn. Mater. **282**, 264 (2004).
[14] C. Z. Wang, G. W. Meng, Q. Q. Fang, X. S. Peng, Y. W. Wang, Q. Fang, and L. D. Zhang, J. Phys. D **35**, 738 (2002).
[15] J. Choi, S. J. Oh, H. Ju, and J. Cheon, Nano Lett. **5**, 2179 (2005).
[16] P. Bruno, Phys. Rev. B **52**, 411 (1995).
[17] D. Stoeffler and F. Gautier, Phys. Rev. B **44**, 10389 (1991).
[18] M. van Schilfgaarde and F. Herman, Phys. Rev. Lett. **71**, 1923 (1993).
[19] P. Lang, L. Nordström, R. Zeller, and P. H. Dederichs, Phys. Rev. Lett. **71**, 1927 (1993).
[20] R. G. Parr and W. Yang, *Density Functional Theory of Atoms and Molecules* (Oxford Science, New York, 1994).
[21] Vienna *ab initio* Simulation Package, Technische Universität Wien, 1999; G. Kresse and J. Furthmüller, Phys. Rev. B **54**, 11169 (1996).
[22] D. E. Ellis, G. A. Benesh, and E. Byrom, Phys. Rev. B **20**, 1198 (1979).
[23] D. D. Sharma, W. Speier, R. Zeller, E. van Leuken, R. A. de Groot, and J. C. Fuggle, J. Phys. C **1**, 9131 (1989).
[24] S. C. Lui, J. W. Davenport, E. W. Plummer, D. M. Zehner, and G. W. Fernando, Phys. Rev. B **42**, 1582 (1990).
[25] W. Lin, Jian-Hua Xu, and A. J. Freeman, J. Mater. Res. **7**, 592 (1992).
[26] J. Zou and C. L. Fu, Phys. Rev. B **51**, 2115 (1995).
[27] H. Y. Geng, N. X. Chen, and M. H. F. Sluiter, Phys. Rev. B **70**, 094203 (2004).
[28] C. Kittel, *Introduction to Solid State Physics* (Wiley, New York, 1953).
[29] P. Weinberger, J. Phys. C **10**, L347 (1977).
[30] G. B. Grad, P. Blaha, K. Schwarz, W. Auwärter, and T. Greber, Phys. Rev. B **68**, 085404 (2003).
[31] F. Liu, M. R. Press, S. N. Khanna, and P. Jena, Z. Phys. D: At., Mol. Clusters **12**, 361 (1989).
[32] P. Panigrahi and R. Pati, Phys. Rev. B **76**, 024431 (2007).
[33] P. W. Anderson, Phys. Rev. **79**, 350 (1950).
[34] T. J. Hicks, B. Rainford, J. S. Kouvel, G. G. Low, and J. B. Comly, Phys. Rev. Lett. **22**, 531 (1969).
[35] C. S. Wang and J. Callaway, Phys. Rev. B **9**, 4897 (1974).
[36] N. Kamakura, Y. Takata, T. Tokushima, Y. Harada, A. Chainani, K. Kobayashi, and S. Shin, Phys. Rev. B **74**, 045127 (2006).
[37] M. Deshpande, D. G. Kanhere, and R. Pandey, Phys. Rev. A **71**, 063202 (2005).